# Sediment transport prediction in sewer pipes during flushing operation

Montes, Carlos; Ortiz, Hachly; Vanegas, Sergio; Kapelan, Zoran; Berardi, Luigi; Saldarriaga, Juan

**DOI**
10.1080/1573062X.2021.1948077

**Publication date**
2021

**Document Version**
Accepted author manuscript

**Published in**
Urban Water Journal

**Citation (APA)**
Montes, C., Ortiz, H., Vanegas, S., Kapelan, Z., Berardi, L., & Saldarriaga, J. (2021). Sediment transport prediction in sewer pipes during flushing operation. *Urban Water Journal*, *19*(1), 1-14. https://doi.org/10.1080/1573062X.2021.1948077

# Sediment Transport Prediction in Sewer Pipes During Flushing Operation

Carlos Montes[a*], Hachly Ortiz[b], Sergio Vanegas[c], Zoran Kapelan[d], Luigi Berardi[e] and Juan Saldarriaga[f]

[a] *Department of Civil and Environmental Engineering, Universidad de los Andes, Bogotá, Colombia; e-mail: cd.montes1256@uniandes.edu.co*

[b] *Department of Civil and Environmental Engineering, Universidad de los Andes, Bogotá, Colombia; e-mail: hv.ortiz@uniandes.edu.co*

[c] *Department of Civil and Environmental Engineering, Universidad de los Andes, Bogotá, Colombia; e-mail: sm.vanegas@uniandes.edu.co*

[d] *Department of Water Management, Delft University of Technology, Delft, Netherlands; e-mail: Z.Kapelan@tudelft.nl*

[e] *Department of Engineering and Geology, Università degli Studi "G. d'Annunzio" Chieti, Pescara, Italy; e-mail: luigi.berardi@unich.it*

[f] *Department of Civil and Environmental Engineering, Universidad de los Andes, Bogotá, Colombia; e-mail: jsaldarr@uniandes.edu.co*

*Corresponding author; Correspondence address: Cra 1 Este No. 19A – 40 Bogota (Colombia); Tel.: +57-1-339-49-49 (ext. 1765)

# Sediment Transport Prediction in Sewer Pipes During Flushing Operation

## Abstract

This paper presents a novel model for predicting the sediment transport rate during flushing operation in sewers. The model was developed using the Evolutionary Polynomial Regression Multi-Objective Genetic Algorithm (EPR-MOGA) methodology applied to new experimental data collected. Using the new model, a series of design charts were developed to predict the sediment transport rate and the required flushing operation time for several pipe diameters. Accurate results (i.e. sediment transport rates) were obtained when applied to a case study in a combined sewer pipe in Marseille, as reported in the literature. The novelty of the model is the inclusion of the pipe slope, the inflow "dam break" hydrograph, and the sediment properties as explanatory parameters. The new model can be used to predict flushing efficiency and design new flushing cleaning schedules in sewer systems.

Keywords: flushing efficiency; sediment transport; sewer cleansing; sewer flushing.

## 1. INTRODUCTION

Sediment deposition and accumulation are well-known issues in sewer systems modelling. The presence of permanent deposits of material at the bottom of sewer pipes produces several problems, such as reduced flow capacity and premature combined sewer overflows (Ashley et al. 2004; Rodríguez et al. 2012). Flushing waves, also known as surge flushing technique, have been identified as an efficient (Bong et al. 2016; Yang et al. 2019) and cost-effective (Campisano et al. 2019, 2007) method for solving these problems. It aims to remove the deposited sediments by generating waves, which are produced by the upstream storage and further discharge of water volumes. These flushing waves increase the bottom shear stress and induce the scour and resuspension of the deposited material.

The above flushing technique has been applied in several case studies following operational and management practice guides (British Standard Institution, 2014; Fan, 2004; Hlavinek et al. 2005; NEIWPCC, 2003) in countries such as Germany, France, the USA and the UK. As an example, Hlavinek et al. (2005) suggest flushing waves to remove settled deposits in sewers ranging from 100 mm to 1200 mm pipe diameter with a mandatory cleaning frequency once in 1 to 5 years. However, these guides do not specify important flushing parameters such as the hydraulic and pipe characteristics (i.e. length, slope and hydraulic roughness, among others), sediment properties and flushing volume. The lack of information on these specifications has contributed to the fact that existing flushing practices tend to be oversized. As an instance, Dettmar (2007) compared design tables developed by using extensive field studies and mathematical simulations (Chebbo et al. 1996; Dettmar, 2005; Lainé et al. 1998) and concluded that smaller flushing volumes and water storage heights achieve the same flushing length and efficiency in removing the volume of deposited sediments, compared to operational and management practice guides.

In the last decades, several studies have quantified the flushing efficiency in terms of: (a) reduction of volume and/or weight of sediments (Bong et al. 2016; Campisano et al. 2019, 2008, 2004; Creaco and Bertrand-Krajewski, 2009; Guo et al. 2004; Ristenpart, 1998; Shahsavari et al. 2017), (b) changes in deposited bed thickness (Bong et al. 2016, 2013a; Campisano et al. 2019, 2008, 2007, 2004; Dettmar et al. 2002; Ristenpart, 1998; Shahsavari et al., 2017; Shirazi et al. 2014), (c) variation of concentrations of total suspended solids (Ristenpart, 1998; Sakakibara, 1996), (d) increase in the bottom shear stress (Bertrand-Krajewski et al. 2003; Campisano et al. 2008; Campisano and Modica, 2003; Dettmar et al. 2002; Ristenpart, 1998; Schaffner and Steinhardt, 2006; Yang et al. 2019), (e) length of the channel that can be potentially cleaned (Bertrand-Krajewski et al. 2003; Bong et al. 2013; Dettmar et al. 2002; Shahsavari et al. 2017; Yang et al. 2019) and (f) stored water volume discharged (Bertrand-Krajewski et al. 2003; Dettmar et al. 2002; Fan et al. 2001). These studies were carried out in both laboratory and real sewer flumes using different sediment characteristics, stored water volumes and geometrical characteristics of the flume. As a result, a list of parameters affecting the flushing efficiency was identified and classified in three main groups: (i) flushing hydraulics, (ii) pipe geometry and (iii) sediment properties. Flushing hydraulic parameters include water velocity ($V_f$), shear stress ($\tau$), the water level in the pipe ($Y$), flowrate ($Q$), stored water head ($h_o$) and stored water volume discharged ($V_a$). In the pipe geometry, parameters as the slope ($S_o$), diameter ($D$), length ($L$), cross-section shape factor ($\beta$) and composite roughness ($k_c$) have been included. Finally, sediment properties include mean particle diameter ($d$), sediment thickness ($y_s$) and width ($W_b$), specific gravity ($SG$), porosity ($\eta$) and density ($\rho_s$).

The previous three groups of parameters have been used for implementing numerical models useful to quantify the flushing efficiency. Models found in the literature are focused on (i) solving complex mathematical structures, (ii) proposing simple dimensionless equations for estimating sediment transport rates and (iii) using Machine Learning (ML) and Artificial Intelligence (AI) techniques for finding patterns in data and predicting bedload and suspended load transport.

In the first approach, the one-dimensional Saint-Venant equations (Campisano et al. 2006; Campisano and Modica, 2003; De Sutter et al. 1999), coupled with the Exner equation for uniform (Campisano et al. 2007, 2004; Creaco and Bertrand-Krajewski, 2009; Shirazi et al. 2014) and non-uniform (Campisano et al. 2019) sediments, are used for predicting bed sediment thickness changes during the flushing operation. More complex models involve the two-dimensional (Caviedes-Voullième et al. 2017; Yu and Duan, 2014) and three-dimensional (Schaffner and Steinhardt, 2006) solutions of the Saint-Venant equations. An example of the literature models is as follows:

$$\frac{\partial U}{\partial t}+\frac{\partial F(U)}{\partial x}=D(U) \tag{1}$$

where $U$, $F(U)$ and $D(U)$ are defined as follows:

$$U=\begin{bmatrix} A \\ Q \\ A_s \end{bmatrix}; F(U)=\begin{bmatrix} Q \\ V_f Q+\frac{F_h}{\rho} \\ \frac{1}{1-\rho}Q_s \end{bmatrix}; D(U)=\begin{bmatrix} 0 \\ gA\left(S_o-\frac{{V_f}^2}{{k_c}^2 R^{4/3}}\right) \\ 0 \end{bmatrix} \tag{2}$$

where $F_h$ is the hydrostatic force over the cross-section, $\rho$ the water density, $R$ the hydraulic radius, $A$ is the cross section wetted area, $A_s$ is the cross-section sediment bed area and $Q_s$ the sediment flow rate.

In the second approach mentioned above, several authors have developed analytical equations for predicting the number of flushes required to move the deposited sediment bed (Bong et al. 2013; Chebbo et al. 1996). Likewise, the effects of pipe slope, bottom roughness, storage water level, and downstream water level, among others (Yang et al. 2019; Kuriqi et al. 2020) have also been studied in the past. As an example, Bong et al. (2013) proposed the following equation, where $n_f$ is the number of flushes required to move the deposited sediment bed by 1 m:

$$n_f=251.43y_s+6.57 \tag{3}$$

In the third approach, several studies using ML and AI have been developed for predicting both bedload and suspended load transport in sewers, flumes, and streams. Several techniques as Artificial Neural Networks (Wan Mohtar et al. 2018; Bajirao et al. 2021), Random Forests (Khosravi et al. 2020; Safari 2020; Montes et al. 2021), and Vector Machines (Ebtehaj et al. 2017), among others, have been trained with experimental data collected at laboratory scale and tested with benchmark data found in the literature. These models outperform traditional regression formulas during the training stage but tend to underperform when applied to external datasets collected in sewers and flumes (Montes et al. 2021), i.e. during the testing stage.

Numerical studies mentioned above, based on the solution of the Saint-Venant and Exner coupled-equations for sediment transport under unsteady flow conditions, show similar predictions of the sediment thickness changes compared to the experimental data collected, i.e. the models show good accuracy prediction. Despite the solutions and simulations based on Saint Venant-Exner equations showing good accuracy, in practice, the application for operational and management practices is complex and non-pragmatic. Also, the analytical and dimensionless equations proposed by Bong et al. (2013) and Yang et al. (2019), do not include important parameters such as the pipe/flume geometry and the sediment characteristics. Finally, AI and ML models are largely black-box models (Montes et al. 2021), limiting their interpretability for practical applications.

The above gaps are addressed here by developing a new parsimonious regression-based model using the Evolutionary Polynomial Regression – Multi-Objective Genetic Algorithm (EPR-MOGA) (Giustolisi and Savic, 2009) strategy. EPR-MOGA is a data-driven method which combines genetic algorithm with evolutionary computing for finding polynomial structures. Due to its characteristics, the returned symbolic expressions can be compared with existing models in terms of the input variables, exponent coefficients, and technical insight on the phenomenon (Montes et al. 2020a) while reducing the risk of overfitting.

This paper aims to propose a new model for predicting the sediment transport rate during flushing operations in sewers. The novelty of this model is the inclusion of flushing "dam break" hydrograph, pipe geometry, and deposited sediment characteristics in a simple polynomial expression. The new model developed here can be used to optimize flushing schemes and reduce the volume of water required for cleaning sewers.

## 2. EXPERIMENTAL METHODS AND DATA COLLECTION

The collection of experimental data was carried out in two pipes with diameters of 209 mm and 595 mm (Montes et al. 2020b), both located at the Hydraulics Laboratory of the University of the Andes, Colombia. A sediment bed with a near-uniform thickness and width was prepared at the bottom of the pipes, using uniformly graded sediment material ranging from 0.21 mm to 2.6 mm. These particles had a specific gravity between 2.57 and 2.67, which was calculated using the pycnometer method (ASTM D854-14, 2014). The experiments were carried out under unsteady flow conditions, simulating the "dam break" waves produced during a flushing event. The methodology used for data collection and further details of both experimental setups are described below.

### *2.1. 209 mm pipe setup*

The 209 mm diameter acrylic pipe had a length of 10.58 m and was supported on six hydraulic jacks, which allowed to vary the pipe slope between 0.64% and 1.20%. This pipe was connected to a 200 mm solenoid valve, which controlled the inflow into the setup from a 3.5 $m^3$ upstream tank. A downstream tank with a V-Notch weir was used to measure the water discharge. A real-time water level sensor was used to measure the water height over the weir to calculate the water discharge rate using the V-Notch equation. The calculated discharge was also checked using an ABB- Electromagnetic flowmeter sensor installed upstream of the pipe. Two additional real-time water level sensors were installed along the pipe, aiming to measure the stage hydrograph produced by the flushing waves. Figure 1 shows the general scheme of the experimental setup.

The experimental data was collected as follows. Firstly, the solenoid valve was fully opened, allowing a base flowrate ranging from 0.002 $\mathrm{l\,s^{-1}}$ to 0.414 $\mathrm{l\,s^{-1}}$. The opening of this valve simulates the 'dam break hydrograph' produced during a flushing operation in a real sewer pipe (e.g. using a Hydrass or a Hydroself flushing gate). Secondly, a sediment bed with near-uniform thickness and width was located at the bottom of the pipe. At this point, the base flowrate helped the formation of the deposited bed along a 3.3 m section. Thirdly, the solenoid valve was completely closed for storing a volume of water between 0.10 $\mathrm{m^3}$ and 0.31 $\mathrm{m^3}$ in the upstream tank. Fourthly, the solenoid valve was opened between 60% and 100% and the opening time was set to 15 sec for all tests. When the first discharged wave reached the sediment bed, the movement of the bed was tracked over time. The sediment velocity ($V_s$) was calculated using the values of the time and deposited bed displacement during the peak flow. The above procedure was repeated for different accumulated upstream water volume and percentage of the solenoid valve opening.

**[Figure 1 near here]**

### *2.2. 595 mm pipe setup*

The pipe was 10.5 m long and supported on a mechanical steel truss, which allowed to modify the slope in a range between 0.04% and 3.44%. The base flow for the experiments, ranging from 1.03 l $s^{-1}$ to 9.98 l $s^{-1}$, was provided by a 40 BHP pump that supplied water to a 30 $m^3$ upstream storage which was directly connected to the pipe. For evaluating unsteady flow conditions in this pipe, a second 10 BHP submersible pump was located inside the downstream tank. This pump was directly connected to the upstream tank and was controlled with a variable frequency drive programmed before the experiment to create a pulse with a maximum peak flow of 30 l $s^{-1}$. Three water level sensors were used to record water depths in the experimental setup. Two of them were installed in the pipe to collect the stage hydrograph, and one was installed in the upstream tank. Full details of the experimental setup were described in Montes et al. (2020b) and are shown in Figure 2.

**[Figure 2 near here]**

For this setup, the data was collected as follows. Firstly, the pipe slope was adjusted using the mechanical steel truss and measured with a dumpy level. Secondly, the flow control valve on the upstream tank was opened to supply a base flow to the pipe. Thirdly, a deposited sediment bed with a near-uniform width was prepared at the bottom of the pipe over a minimum length of 1.5 m. At this point, to compare the flushing efficiency under similar conditions, the maximum sediment bed velocity was verified as 0.03 m $s^{-1}$. If this condition was not fulfilled, the pipe slope or the base flow were changed. Fourthly, the submersible pump, with its variable frequency drive, was activated to simulate the ‘dam break hydrograph’, which is similar to those produced by the flushing gates in real sewers. The water levels were recorded each 0.025 sec and the position of the sediment bed was tracked. The sediment velocity was calculated using the same procedure followed on the acrylic setup.

### *2.3. Experimental data collected*

Using the experimental rig and approach described above, a total of 57 and 64 experiments were carried out in the 209 mm acrylic pipe and 595 mm PVC pipe, respectively. Several variables related to the pipe geometry, sediment properties, and flushing hydraulics, including the base time ($t_b$), peak time ($t_p$), base flow ($Q_b$), and peak flow ($Q_p$) were recorded in each experiment, as shown in Figure 3. The experimental data collected in both acrylic and PVC pipes are presented in Table 1, where $S_o$ is the pipe slope, $D$ the pipe diameter, $Y$ the water level in the pipe, $R$ the hydraulic radius, $d$ the mean particle diameter, $SG$ the specific gravity, $y_s$ the sediment thickness, $V_f$ the water velocity, and $V_s$ the sediment velocity.

**[Figure 3 near here]**

**[Table 1 near here]**

A flushing discharge hydrograph and a plot showing the sediment bed position related with each run are presented in Table 1. The shape and magnitude of the hydrograph are directly related to the sediment bed velocity, and consequently, the sediment bed position. As an example, for six runs, the variation in the sediment bed position and hydrograph characteristics, in both acrylic and PVC pipe, are presented in Figure 4. Full details of each run shown in Figure 4 are presented in Table 1.

**[Figure 4 near here]**

Figure 4A and Figure 4B show the relation between the flushing discharge hydrograph and the sediment bed position for tests conducted on the acrylic pipe. As seen in these figures, particle size is a more important variable in defining the sediment position, compared to the peak flow in the hydrograph. Even though the run 82 considers a higher peak flow ($Q_p$ = 5.55 l s$^{-1}$), the final position of the sediment bed (= 0.41 m) is lower than the run 96 (= 2.62 m) when the peak flow is lower ($Q_p$ = 2.08 l s$^{-1}$). This occurs because the particle diameter is more relevant compared to the peak flow.

Figure 4C and Figure 4D show the relation between the flushing discharge hydrograph and the sediment bed position for tests in 595 mm setup. The relationship between the discharge hydrograph and the sediment bed position is proportional. For run no. 36 and 61, the mean particle diameter was 2.60 mm, but the pipe slope was 1.65% and 1.82%, respectively. Figure 4D shows that maintaining the mean particle diameter constant as the pipe slope increases, the final bed position increases.

# 3. MODEL DEVELOPMENT

## *3.1. Graphical analysis*

A graphical analysis was developed to visualize the relationships between the variables collected in each experiment. The relationship between sediment velocity and flow velocity ($V_s/V_f$) was plotted against other dimensionless parameters, as shown in Figure 5. These dimensionless parameters have been previously identified as relevant for predicting sediment transport in sewer pipes in previous literature (Ab Ghani and Azamathulla, 2011; Ebtehaj and Bonakdari, 2016; May et al. 1996; Kuriqui et al. 2020; Montes et al. 2021). Two of these parameters include the dimensionless grain size ($d/R$) and the Shields parameter ($\psi$), defined in Eq. (4):

$$\psi = \frac{RS_o}{(SG-1)d} \tag{4}$$

Based on the results shown in Figure 5, the following observations can be made:

- In general, higher values of the Shields parameter lead to higher values of $V_s/V_f$. This can be clearly seen in the acrylic pipe (Figure 5a) because of the constant slope value adopted in the experimental rig. Furthermore, high values of $S_o$ and $R$ lead to higher sediment velocities due to higher critical shearing stress (i.e. the applied forces are higher than the submerged weight of the particle). In contrast, deposited materials with high density of particle diameters result in lower sediment velocities.
- The direct relationship between $V_s/V_f$ and the Shields parameter coincides with the inversely proportional relationship between $V_s/V_f$ and $d/R$, shown in Figure 5c and Figure 5d. This is observed because the Shields parameter includes the ratio $R/d$, as shown in Eq. (4).
- Figure 5e shows the inversely proportional relationship between $V_s/V_f$ and the dimensionless parameter $Q_b/Q_p$, meaning that higher and steeper discharge hydrographs (i.e. lower ratios $Q_b/Q_p$) show higher $V_s/V_f$ values.
- In general, based on what was previously mentioned, higher values of $S_o$ and $R$ and lower values of $d$, $SG$, and $Q_b/Q_p$ lead to higher sediment velocities $V_s$.

**[Figure 5 near here]**

### *3.2. Evolutionary Polynomial Regression model*

A new regression-based model was developed here to predict the dimensionless ratio $V_s/V_f$ during flushing operation. The new model includes the group of parameters identified in previous studies (Ab Ghani and Azamathulla, 2011; Ebtehaj and Bonakdari, 2016; May et al. 1996; Montes et al. 2021) and the graphic analysis carried out for the experimentally collected data, as shown in Figure 5.

Evolutionary polynomial regression (EPR) is a hybrid regression technique that combines numerical and symbolic regression (Giustolisi and Savic, 2006, 2004). In its original formulation, it used single objective genetic algorithms to explore the formula space, and then it estimates the least-squares regression coefficients. This technique has proved to be effective when the number of polynomial terms is not large (Giustolisi and Savic, 2009). To solve these issues, Giustolisi and Savic (Giustolisi and Savic, 2009) introduced the EPR technique combined with a Multi-Objective Genetic Algorithm (MOGA). This novel technique maximises the model accuracy (i.e. minimises the sum of squared errors) and minimises the number of polynomial coefficients, and therefore improves the exploration of the space of symbolic formulas. EPR-MOGA considers some pseudo-polynomial expressions such as (Giustolisi and Savic, 2009):

$$\widehat{\boldsymbol{Y}} = a_0 + \sum_{j=1}^{m} a_j (\boldsymbol{X_1})^{ES(j,1)} \cdot \ldots \cdot (\boldsymbol{X_k})^{ES(j,k)} \cdot f\left((\boldsymbol{X_1})^{ES(j,k+1)}\right) \cdot \ldots \cdot f\left((\boldsymbol{X_k})^{ES(j,2k)}\right) \tag{5}$$

where $\widehat{\boldsymbol{Y}}$ is the vector of model predictions; $ES$ and $j$ the matrix of candidate exponents and the inner function, respectively, both selected by the user; $m$ the number of terms; $a_0$ the bias term; $a_j$ the adjustable parameters estimated by linear least squares and $\boldsymbol{X_j}$ the candidate explanatory variables. The inner function $f$ defined by the user can be logarithmic, exponential, tangent hyperbolic, or secant hyperbolic, and must be selected according to the physics of the problem studied. The EPR technique returns a range of models showing the influence of different explanatory factors by progressively adding these as input variables to monomial formulas, starting from the most important ones. For each EPR identified model, the following performance indices are calculated: the Bayesian Information Criterion ($BIC$) and the Coefficient of Determination ($R^2$), as shown in Eq. (6) and Eq. (7), respectively.

$$BIC = \left(1 + d\frac{\log(n)}{n}\right)\left(\sum_{i=1}^{n}(Y^* - Y)^2\right) \tag{6}$$

$$R^2 = 1 - \frac{\sum_{i=1}^{n}(Y^* - Y)^2}{\sum_{i=1}^{n}(Y^* - \overline{Y^*})^2} \tag{7}$$

where $Y^*$ and $Y$ are the observed and calculated data, respectively, $n$ is the number of data, $d$ the number of parameters included in the model and $\overline{Y^*}$ the mean of observed data. The Coefficient of Determination measures the fraction of variance that can be explained. Note that this coefficient varies between 0 and 1, where 1 denotes a perfect match between observed and calculated data. The Bayesian Information Criterion measures the trade-off between accuracy and parsimony of the model. This measure penalises formulas with large number of parameters. The model with the lowest BIC value is selected as optimal.

The new model was constructed to predict the dimensionless relation $V_s/V_f$, i.e. the vector of model predictions $\widehat{\boldsymbol{Y}}$ is defined as $V_s/V_f$. The matrix of candidate exponents was defined with values ranging from -2.50 to 2.50, considering steps of 0.1, i.e. $ES = [-2.50, -1.40, \dots, 1.40, 2.50]$. The matrix of candidate explanatory variables is defined as follows:

$$\boldsymbol{X_j} = \left[\psi, \frac{d}{R}, \frac{Q_b}{Q_p}, \frac{y_s}{R}, \frac{t_b}{t_p}, \beta\right] \tag{8}$$

Using previous considerations, and randomly splitting the experimental data collected on the 209 mm and 595 mm pipes, for both training (75% of the data) and testing (25% of the data) stages, the results shown in Table 2 were obtained using the EPR-MOGA strategy.

**[Table 2 near here]**

Table 2 shows the Pareto front (i.e. range of models) generated by the EPR, together with the corresponding $BIC$ and $R^2$ values. For example, the best 1 input variable model includes only the Shields parameter as an explanatory variable for predicting the $V_s/V_f$ ($V_s/V_f = 0.17\psi^{0.5}$). This is the least complex, i.e. most parsimonious model hence, unsurprisingly, it has a rather low prediction accuracy ($BIC$ = -48.21 and $R^2$ = 0.38). In contrast, the 6-variable model includes all candidate explanatory factors $\left(V_s/V_f = 2.48\psi^{1.4}\left(\frac{Q_b}{Q_p}\right)^{-0.3}\left(\frac{d}{R}\right)^{0.9}\left(\frac{y_s}{R}\right)^{0.1}\left(\frac{t_b}{t_p}\right)^{-0.2}\beta\right)$, resulting in low parsimony model but with improved prediction accuracy ($BIC$ = -92.22 and $R^2$ = 0.64). Based on this, the model that shows the best trade-off between accuracy and parsimony is the model with 3 input variables. This model is shown in Eq. (9).

$$\frac{V_s}{V_f} = 8.13\left(\frac{d}{R}\right)^{0.90}\left(\frac{RS_o}{(SG-1)d}\right)^{1.40}\left(\frac{Q_b}{Q_p}\right)^{-0.30} \tag{9}$$

Or rearranging the above formula to simplify the $d/R$ term:

$$\frac{V_s}{V_f} = 8.13\left(\frac{d}{R}\right)^{-0.50}\left(\frac{S_o}{(SG-1)}\right)^{1.40}\left(\frac{Q_b}{Q_p}\right)^{-0.30} \tag{10}$$

The obtained model was used to estimate the flushing efficiency in larger pipes considering different flow conditions and sediment characteristics. Further details are described in the section below. The model's accuracy can be seen in Figure 6 for both training and testing datasets.

**[Figure 6 near here]**

As it can be seen from the above equation and figure, Eq. (10) is consistent with the graphical analysis presented in Figure 6. Further, it can be seen from the model obtained that $\frac{S_o}{(SG-1)}$ is the most important feature for predicting the sediment velocity during the flushing cleaning operation - the more the pipe slope increases, the higher the particle velocity is (note that the $\frac{S_o}{(SG-1)}$ parameter comes from the Shields parameter). The Shields parameter shows the ratio between the hydrodynamic forces acting on the particles and the resistance due to gravity. This parameter has been identified as one of the most relevant for predicting the incipient motion in sewers (Delleur, 2001; Safari et al. 2018; Wan Mohtar et al. 2018). As mentioned above, $V_s/V_f$ is inversely proportional to $d/R$, which is consistent with the results shown by EPR-MOGA model.

## 4. RESULTS AND DISCUSSION

The new model shown in Eq. (10) was used to generate charts to estimate flushing efficiency as a function of the characteristics of the discharged hydrograph, the pipe geometry and the sediment properties. In this context, two flushing-efficiency measures were defined as a function of the area of deposited bed ($A_s$) and the sediment velocity. The first measure, $Q_s$, is the volume of sediment removed by unit time (i.e. the sediment flow rate = $A_s V_s$). The second measure, $t_e$, is the flushing time required to clean 1.0 m of the pipe (= $1/V_s$). Figure 7 and Figure 8 were constructed for several pipe diameters using previous measures. To construct these figures, the less-significant variables identified by the EPR-MOGA model (as shown in Table 2) remained constant. The sediment thickness was defined as $y_s/D = 1\%$, the specific gravity of the sediments as 2.6, and the relation between the base and peak time of the hydrograph as $t_b/t_p = 5.0$.

**[Figure 7 near here]**

The following observations can be made from Figure 7 and Figure 8:

- $Q_s$ is inversely proportional to $d$ and $Q_b/Q_p$. In addition, $Q_s$ seems to be near-steady for particle diameters greater than 1.5 mm in pipes with diameters less than

800 mm. All above for the same pipe slope and $Q_b/Q_p$ relation. Increasing the pipe slope directly increase the sediment transport rate.

- As the $Q_b/Q_p$ ratio increases, the sediment removal rate decreases. For example, in Figure 7a, when $Q_b/Q_p$ = 0.25 in a 1200 mm diameter pipe containing a deposited sediment bed with $d$ = 1 mm, $Q_s$ = 0.5 ×10$^{-4}$ m$^3$/s, while for $Q_b/Q_p$ = 0.75 the $Q_s$ value changes to 0.2 ×10$^{-4}$ m$^3$/s, that is 60% less (as shown in Figure 7c).
- Flushing discharges seem to be more efficient in larger sewer pipes. The sediment transport rate can be five times higher in 2000 mm diameter pipes, compared to 1200 mm diameter pipes.
- Figure 8 shows a direct relationship between $t_e$ and $d$ and $Q_b/Q_p$. Based on this, as $d$ increases and $Q_p$ decreases, the required flushing time to clean 1 meter of the pipe increases. For example, in Figure 8d when $Q_b/Q_p$ = 0.25 in a 800 mm diameter pipe containing a deposited sediment bed with $d$ = 1.5 mm, $t_e$ = 20 sec, while for $Q_b/Q_p$ = 0.75 the $t_e$ value changes to 45 sec, that is 125% more (as shown in Figure 8f)
- The flushing time decreases as the $S_o$ and $D$ increase. That is, flushing is a more efficient technique in large and steep pipes.

**[Figure 8 near hear]**

### *4.1. Model comparison*

To test the accuracy of the model shown in Eq. (10), the case study described in Laplace et al. (2003) was used. This case study is located in Marseille, France, on a combined sewer network. Specifically, this study considers an ovoid section of 1700 mm, 120 m long with a bottom slope of 0.03%. A near-uniform deposited bed of 140 mm thickness was observed along the entire length of the flume. The deposited bed was characterised as coarser upstream ($d$ = 8 mm) and finer downstream ($d$ = 0.6 mm). Full details are shown in Laplace et al. (2003).

Using a Hydrass-flushing gate located inside the section, a series of flushes were conducted for testing the efficiency on removing the deposited material. During each flush, a total volume of 6.0 m$^3$ of water was discharged into the pipe. As reported by Laplace et al. (2003), the mass of particles eroded during the first flush was 6.3 kg, i.e. the removal rate was 1.08 kg of material per 1.0 m$^3$ of water (= 1.08 kg m$^{-3}$).

Two existing procedures are compared with the new EPR-MOGA model presented in Eq. (10): the model proposed by Bong et al. (2013) (i.e. Eq. (3)) and the design tables shown by Dettmar (2007). To compare the results, several initial conditions are defined based on the case study description, which are outlined as follows:

(1) Thickness of the deposited bed ($y_s$) = 0.14 m
(2) Peak flow during flushing operation ($Q_p$) = 100 l s$^{-1}$
(3) Specific gravity of the sediments ($SG$) = 2.60
(4) Mean particle diameter ($d$) = 0.6 – 8.0 mm
(5) Mass of material per meter of pipe = 54.22 kg m$^{-1}$

According to Bong et al. (2013), the number of flushes required to move 1 m of deposited material can be estimated by applying Eq. (3). For this equation, the number of flushes is only a function of the thickness of the deposited bed. As a result, 42 flushes (= 250.6 m$^3$ of water) can potentially remove 54.22 kg of the deposited material (i.e. the removal rate is 0.21 kg m$^{-3}$). Design tables proposed by Dettmar (2007) suggest a flushing volume of 48 $m^3$ for a basic cleaning of the 150 m long sewer (i.e. a full removing of the deposited material). No removal rates are provided by Dettmar (2007).

Finally, using the new model proposed in this study, a range of removal rates are obtained as a function of the mean particle diameter. Potentially, a flushing volume of 10.18 $m^3$ can remove 14.5 kg of deposited material with a mean particle diameter of 0.6 mm (i.e. the removal rate is 0.40 kg $m^{-3}$). By changing the particle size of the deposited material to 8.3 mm, the removal rate is 1.25 kg $m^{-3}$.

**[Table 3 near here]**

As shown in Table 3, a direct comparison of the method proposed by Dettmar (2007) and the results reported by Laplace et al. (2003) is not possible. However, this method seems to underestimate the real volume required to remove the deposited bed. Relevant parameters such as the mean particle diameter and the sewer hydraulics are not included in this method. Due to the pipe slope in the case of study is almost flat, obtaining minimum shear stress of 5.0 N $m^{-2}$ for cleaning the pipe, according to Dettmar (2007), requires larger flows.

The model presented by Bong et al. (2013) is a good approach for determining the number of flushes required to move the deposited material. However, because of the non-inclusion of relevant pipe hydraulics and sediment parameters, the results are underestimated, compared to the values reported by Laplace et al. (2003).

### *4.2. Model considerations*

The new model presented here shows good prediction accuracy with the data reported by Laplace et al. (2003). This is explained by the inclusion of relevant parameters for predicting the removal rate during the flushing operation. The model also shows good extrapolation capabilities under different sewer diameters and a wide range of variations of the mean particle diameter.

The Shields parameter was selected as the most important one due to the highest value in the regression coefficient and the Pareto solution provided by the EPR-MOGA strategy. This was expected since this parameter determines the threshold condition of sediment initiation motion. The sediment thickness parameter is less important for defining the sediment velocity during the flushing operation due to the low regression coefficient presented in Table 2. As a result, the model can be used in both combined and storm sewers, where the sediment thickness ranges from 10 mm to 100 mm and 10 mm to 330 mm, respectively (Bong et al. 2016).

The model includes the peak flow as an explanatory variable for predicting sediment transport rate. Higher peak flow implies a higher removal rate since higher shear stresses are generated at the bottom of the pipe. The observed shear stress values (ranging from 2.0 N/m$^2$ to 6.5 N/m$^2$ in the PVC pipe) are consistent with those reported in the literature for the erosion and transport of bed material (Dettmar, 2007; Campisano et al. 2008; Yang et al. 2019). However, since the model only considers transport as bedload, some fine particles may be eroded and transported in suspension (which has been identified as one of the major sources of pollution in CSO (Laplace et al. 2003; Saul et al. 2003)), due to the high turbulence of the flow. This is particularly important in well-graded materials where wide ranges of mean particle sizes are present.

Even though the new model was developed considering a wide range of variations in input variables, some limitations exist. The granular material used in the experiments cannot represent the cohesive properties of sediments found in real sewer systems. As a result, an increased bed resistance to erosion can be seen in practice (Campisano et al.

2019). In addition, the lowest pipe slope value considered during the tests was 0.644%, which is higher than the minimum self-cleansing value recommended in several industry design codes and water utilities design manuals (e.g. Health Research Inc. (2004), as quoted by Montes et al. (2019)).

## 5. CONCLUSIONS

This study proposes a simple model to predict the sediment transport rate in practice based on data collected from a set of 121 lab experiments conducted on a 209 mm diameter acrylic pipe and 595 mm diameter PVC pipe. The data collected this way were processed using the EPR-MOGA modelling technique. A new model for predicting the sediment velocity during flushing operation was developed and used for constructing design charts. Based on the results obtained, the following conclusions are made:

(1) The new model developed and presented here can predict the sediment transport rate during flushing discharges accurately in practice. This model includes the group of parameters that most affect the flushing efficiency in sewer pipes.

(2) The sediment transport rate is principally affected by four parameters: pipe slope, pipe diameter, particle diameter and discharged peak flow. In pipes with large diameters and slopes, the flushing is more effective. This is because of the high regression exponents for both $\frac{S_o}{(SG-\ )}$ and $d/R$ variables obtained in the EPR-MOGA model presented here. The sediment transport is not significantly affected by the value of the deposited sediment thickness.

(3) The new model proposed outperforms the simplified models and methods reported in the literature in terms of removal sediment rate prediction. This is seen by the better prediction accuracy shown when compared to the case study reported by Laplace et al. (2003).

(4) Existing models such as Bong et al. (2013) and Dettmar (2007) for predicting sediment transport tend to underestimate the total volume of water required to clean a deposited sediment bed. The EPR-MOGA model is more accurate in predicting the sediment transport rate as this model includes parameters affecting the flushing efficiency, such as flushing hydraulics, pipe geometry and sediment properties.

Based on the conclusions mentioned above, the new flushing model can be useful for designing flushing schemes during the operational stage of existing sewer pipes in engineering practice. Further research is recommended to test the model proposed in real sewer pipes under different sediment (i.e. cohesive materials) and hydraulic conditions.

## Acknowledgements

The authors would like to thank Professor Orazio Giustolisi who developed and made available for free the EPR software used in this research.

## Disclosure Statement

No potential conflict of interest was reported by the author(s).

## Funding

This research received no external funding.

## REFERENCES

Ab Ghani, A., and Azamathulla, H. 2011. “Gene-Expression Programming for Sediment Transport in Sewer Pipe Systems.” *Journal of Pipeline Systems Engineering and Practice* 2(3): 102–106. https://doi.org/10.1061/(ASCE)PS.1949-1204.0000076

Ashley, R., Bertrand-Krajewski, J., Hvitved-Jacobsen, T., and Verbanck, M., 2004. *Solids in Sewers: Characteristics, Effects and Control of Sewer Solids and Associated Pollutants*. London: IWA Publishing. https://doi.org/10.2166/9781780402727

ASTM D854-14, 2014. *Standard Test Methods for Specific Gravity of Soil Solids by*

*Water Pycnometer*. West Conshohocken, PA: ASTM International.

Azamathulla, H., Ab Ghani, A., and Fei, S., 2012. “ANFIS-based approach for predicting sediment transport in clean sewer.” *Applied Soft Computing Journal* 12(3): 1227–1230. https://doi.org/10.1016/j.asoc.2011.12.003

Bajirao, T., Kumar, P., Kumar, M., Elbeltagi, A., and Kuriqi, A. 2021. “Superiority of Hybrid Soft Computing Models in Daily Suspended Sediment Estimation in Highly Dynamic Rivers.” *Sustainability* 13(2): 542. https://doi.org/10.3390/su13020542

Bertrand-Krajewski, J., Bardin, J., Gibello, C., and Laplace, D. 2003. “Hydraulics of a sewer flushing gate.” *Water Science and Technology* 47(4), 129–136. https://doi.org/10.2166/wst.2003.0237

Bong, C., Lau, T., and Ab Ghani, A. 2016. “Potential of tipping flush gate for sedimentation management in open stormwater sewer.” *Urban Water Journal* 13(5): 486–498. https://doi.org/10.1080/1573062X.2014.994002

Bong, C., Lau, T., Ab Ghani, A., and Chan, N. “Sediment deposit thickness and its effect on critical velocity for incipient motion.” *Water Science and Technology* 74(8): 1876-1884. https://doi.org/10.2166/wst.2016.376

Bong, C., Lau, T., and Ab Ghani, A. 2013. “Hydraulics characteristics of tipping sediment flushing gate.” *Water Science and Technology* 68(11): 2397–2406. https://doi.org/10.2166/wst.2013.498

British Standard Institution, 2014. *Management and Control of Operational Activities in Drain and Sewer Systems Outside Buildings. Part 1: Cleaning*. London, UK.

Campisano, A., Creaco, E., and Modica, C. 2008. “Laboratory investigation on the effects of flushes on cohesive sediment beds.” *Urban Water Journal* 5(1): 3–14. https://doi.org/10.1080/15730620701726259

Campisano, A., Creaco, E., and Modica, C. 2007. “Dimensionless Approach for the Design of Flushing Gates in Sewer Channels.” *Journal of Hydraulic Engineering* 133(8): 964–972. https://doi.org/10.1061/(ASCE)0733-9429(2007)133:8(964)

Campisano, A., Creaco, E., and Modica, C. 2006. “Experimental analysis of the hydrass flushing gate and laboratory validation of flush propagation modelling.” *Water Science and Technology* 54(6-7): 101–108. https://doi.org/10.2166/wst.2006.608

Campisano, A., Creaco, E., and Modica, C. 2004. “Experimental and numerical analysis of the scouring effects of flushing waves on sediment deposits.” *Journal of Hydrology* 299(3-4): 324–334. https://doi.org/10.1016/j.jhydrol.2004.08.009

Campisano, A., and Modica, C. 2003. “Flow velocities and shear stresses during flushing operations in sewer collectors.” *Water Science and Technology* 47(4): 123–128. https://doi.org/10.2166/wst.2003.0236

Campisano, A., Modica, C., Creaco, E., and Shahsavari, G. 2019. “A model for non-uniform sediment transport induced by flushing in sewer channels.” *Water Research* 163: 114903. https://doi.org/10.1016/j.watres.2019.114903

Caviedes-Voullième, D., Morales-Hernández, M., Juez, C., Lacasta, A., and García-Navarro, P. 2017. “Two-dimensional numerical simulation of bed-load transport of a finite-depth sediment layer: Applications to channel flushing.” *Journal of Hydraulic Engineering* 143(9):04017034. https://doi.org/10.1061/(ASCE)HY.1943-7900.0001337

Chebbo, G., Laplace, D., Bachoc, A., Sanchez, Y., and Le Guennec, B. 1996. “Technical solutions envisaged in managing solids in combined sewer networks.” *Water Science and Technology* 33(9): 237–244. https://doi.org/10.1016/0273-1223(96)00392-7

Creaco, E., and Bertrand-Krajewski, J. 2009. “Numerical Simulation of flushing effect on sewer sediments and comparison of Four sediment transport formulas.” *Journal of Hydraulic Research* 47(2): 195–202. https://doi.org/10.3826/jhr.2009.3363

De Sutter, R., Huygens, M., and Verhoeven, R. 1999. “Unsteady flow sediment transport in a sewer model.” *Water Science and Technology* 39(9): 121–128. https://doi.org/10.1016/S0273-1223(99)00224-3

Delleur, J. 2001. “New results and research needs on sediment movement in urban drainage.” *Journal of Water Resources Planning and Management* 127(3): 186-193. https://doi.org/10.1061/(ASCE)0733-9496(2001)127:3(186)

Dettmar, J. 2007. “A new planning procedure for sewer flushing.” Paper presented at the NOVATECH 2007 – Sixth International Conference on Sustainable Techniques and Strategies in Urban Water Management, Lyon, June 25-28.

Dettmar, J. 2005. “Beitrag zur Verbesserung der Reinigung von Abwasserkanälen.” PhD diss., RWTH Aachen University.

Dettmar, J., Rietsch, B., and Lorenz, U. 2002. “Performance and Operation of Flushing Devices - Results of a Field and Laboratory Study.” *Global Solutions for Urban Drainage: Proceedings of the Ninth International Conference on Urban Drainage*: 1–10. https://doi.org/10.1061/40644(2002)291

Ebtehaj, I., and Bonakdari, H. 2016. “Bed Load Sediment Transport in Sewers at Limit of Deposition.” *Scientia Iranica* 23(3): 907–917. https://doi.org/10.24200/sci.2016.2169

Ebtehaj, I., Bonakdari, H., Shamshirband, S., Ismail, Z., and Hashim, R. 2017. “New approach to estimate velocity at limit of deposition in storm sewers using vector machine coupled with firefly algorithm.” *Journal of Pipeline Systems Engineering and Practice* 8(2): 04016018. https://doi.org/10.1061/(ASCE)PS.1949-1204.0000252

Fan, C. 2004. *Sewer Sediment and Control A Management Practices Reference Guide*. U.S. Environmental Protection Agency, Washington, DC, EPA/600/R-04/059.

Fan, C., Field, R., Pisano, W., Barsanti, J., Joyce, J., and Sorenson, H. 2001. “Sewer and Tank Flushing for Sediment, Corrosion, and Pollution Control.” *Journal of Water Resources Planning and Management* 127(3): 194–201.

https://doi.org/10.1061/(ASCE)0733-9496(2001)127:3(194)

Giustolisi, O., and Savic, D. 2009. “Advances in data-driven analyses and modelling using EPR-MOGA.” *Journal of Hydroinformatics* 11(3-4): 225–236. https://doi.org/10.2166/hydro.2009.017

Giustolisi, O., and Savic, D. 2006. “A symbolic data-driven technique based on evolutionary polynomial regression.” *Journal of Hydroinformatics* 8(4): 207–222. https://doi.org/10.2166/hydro.2006.020

Giustolisi, O., and Savic, D. 2004. “A Novel Genetic Programming Strategy: Evolutionary Polynomial Regression.” *Proceedings of the 6th International Conference on Hydroinformatics*: 787–794. https://doi.org/10.1142/9789812702838_0097

Guo, Q., Fan, C., Raghaven, R., and Field, R. 2004. “Gate and Vacuum Flushing of Sewer Sediment: Laboratory Testing.” *Journal of Hydraulic Engeneering* 130(5): 463–466. https://doi.org/10.1061/(ASCE)0733-9429(2004)130:5(463)

Health Research Inc. (2004). “Recommended standards for wastewater facilities.” *A Report of the Wastewater Committee* 12224(518): 1–102.

Hlavinek, P., Malanik, S., Raclavsky, J., Sulcova, V., Montero, C., and Villanueva, A. 2005. *WP4 Deliverable 11: Survey of Operational Options*. Brno.

Khosravi, K., Cooper, J., Daggupati, P., Thai Pham, B., and Tien Bui, D. 2020. “Bedload transport rate prediction: Application of novel hybrid data mining techniques” *Journal of Hydrology* 585: 124774 https://doi.org/10.1016/j.jhydrol.2020.124774

Kuriqui, A., Koçileri, G., and Ardiçlioğlu, M. 2020. “Potential of Meyer-Peter and Müller approach for estimation of bed-load sediment transport under different hydraulic regimes” *Modeling Earth Systems and Environment* 6: 129-137. https://doi.org/10.1007/s40808-019-00665-0

Lainé, S., Phan, L., Malabat, D., and Duffros, B. 1998. “Flush Cleaning of Sewer Using the Hydras-Valve.” Paper presented at the 4th International Conference on Urban Drainage Modelling, London, September 21-24.

Laplace, D., Oms, C., Ahyerre, M., Chebbo, G., Lemasson, J., and Felouzis, L. 2003. “Removal of the organic surface layer in combined sewer sediment using a flushing gate.” *Water Science and Technology* 47(4): 19–26. https://doi.org/10.2166/wst.2003.0211

May, R., Ackers, J., Butler, D., and John, S. 1996. “Development of design methodology for self-cleansing sewers.” *Water Science and Technology* 33(9): 195–205. https://doi.org/10.1016/0273-1223(96)00387-3

Montes, C., Bohorquez, J., Borda, S., and Saldarriaga, J. 2019. “Impact of Self-Cleansing Criteria Choice on the Optimal Design of Sewer Networks in South America.” *Water (Switzerland)* 11(6): 1148. https://doi.org/10.3390/w11061148

Montes, C., Berardi, L., Kapelan, Z., and Saldarriaga, J. 2020a. “Predicting bedload sediment transport of non-cohesive material in sewer pipes using evolutionary polynomial regression – multi-objective genetic algorithm strategy." *Urban Water Journal* 17(2): 154-162. https://doi.org/10.1080/1573062X.2020.1748210

Montes, C., Vanegas, S., Kapelan, Z., Berardi, L., and Saldarriaga, J. 2020b. "Non-deposition self-cleansing models for large sewer pipes." *Water Science and Technology* 81(3): 606–621. https://doi.org/10.2166/wst.2020.154

Montes, C., Kapelan, Z., and Saldarriaga, J. 2021. "Predicting non-deposition sediment transport in sewer pipes using Random forest." *Water Research* 189, 116639. https://doi.org/10.1016/j.watres.2020.116639

NEIWPCC, 2003. Optimizing Operation, Maintenance, and Rehabilitation of Sanitary Sewer Collection Systems. Lowell, MA.

Ristenpart, E. 1998. "Solids transport by flushing of combined sewers." *Water Science and Technology* 37(1): 171–178. https://doi.org/10.1016/S0273-1223(97)00767-1

Rodríguez, J., McIntyre, N., Díaz-Granados, M., and Maksimović, Č. 2012. "A database and model to support proactive management of sediment-related sewer blockages." *Water Research* 46(15): 4571–4586. https://doi.org/10.1016/j.watres.2012.06.037

Safari, M. 2020. "Hybridization of multivariate adaptive regression splines and random forest models with an empirical equation for sediment deposition prediction in open channel flow." *Journal of Hydrology* 590: 125392. https://doi.org/10.1016/j.jhydrol.2020.125392

Safari, M., Mohammadi, M., and Ab Ghani, A. 2018. "Experimental studies of self-cleansing drainage system design: A review." *Journal of Pipeline Systems Engineering and Practice* 9(4): 04018017. https://doi.org/10.1061/(ASCE)PS.1949-1204.0000335

Sakakibara, T. 1996. "Sediments flushing experiment in a trunk sewer." *Water Science and Technology* 33(9): 229–235. https://doi.org/10.1016/0273-1223(96)00391-5

Saul, A., Skipworth, P., Tait, S., and Rushforth, P. 2003. "Movement of Total Suspended Solids in Combined Sewers." *Journal of Hydraulic Engineering* 129(4): 298-307. https://doi.org/10.1061/(ASCE)0733-9429(2003)129:4(298)

Schaffner, J., and Steinhardt, J. 2006. "Numerical investigation of the self-acting flushing system HydroFlush GS in Frankenberg/Germany." Paper presented at the 2th Conference on Sewer Operation and Maintenance, Vienna, October.

Shahsavari, G., Arnaud-Fassetta, G., and Campisano, A. 2017. "A field experiment to evaluate the cleaning performance of sewer flushing on non-uniform sediment deposits." *Water Research* 118: 59–69 https://doi.org/10.1016/j.watres.2017.04.026

Shirazi, R., Campisano, A., Modica, C., and Willems, P. 2014. "Modelling the erosive effects of sewer flushing using different sediment transport formulae." *Water Science and Technology* 69(6): 1198–1204. https://doi.org/10.2166/wst.2013.810

Wan Mohtar, W., Afan, H., El-Shafie, A., Bong, C., and Ab Ghani, A. 2018. "Influence of bed deposit in the prediction of incipient sediment motion in sewers using artificial neural networks.” *Urban Water Journal* 15(4): 296-302. https://doi.org/10.1080/1573062X.2018.1455880

Yang, H., Zhu, D., Zhang, Y., and Zhou, Y. 2019. “Numerical investigation on bottom shear stress induced by flushing gate for sewer cleaning.” *Water Science and Technology* 80(2): 290–299. https://doi.org/10.2166/wst.2019.269

Yu, C., and Duan, J. 2014. “Two-Dimensional Finite Volume Model for Sediment Transport in Unsteady Flow.” *World Environmental and Water Resources Congress 2014*: 1432–1441. https://doi.org/10.1061/9780784413548.144

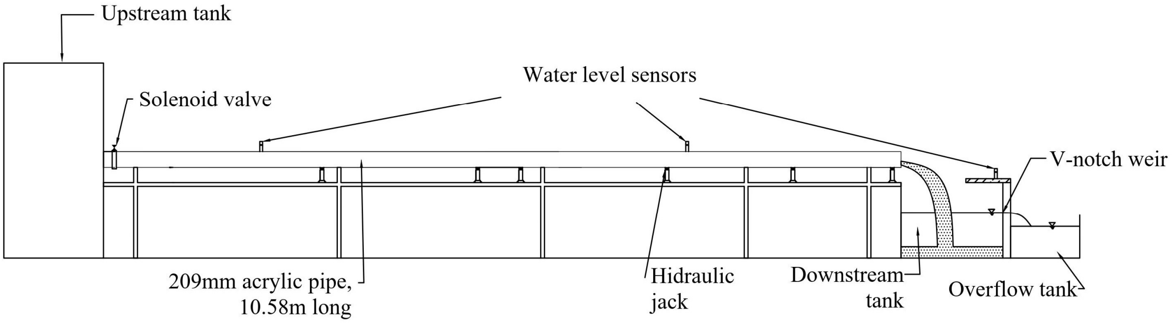

Figure 1. Experimental setup used to collect the unsteady flow data in the 209 mm acrylic pipe.

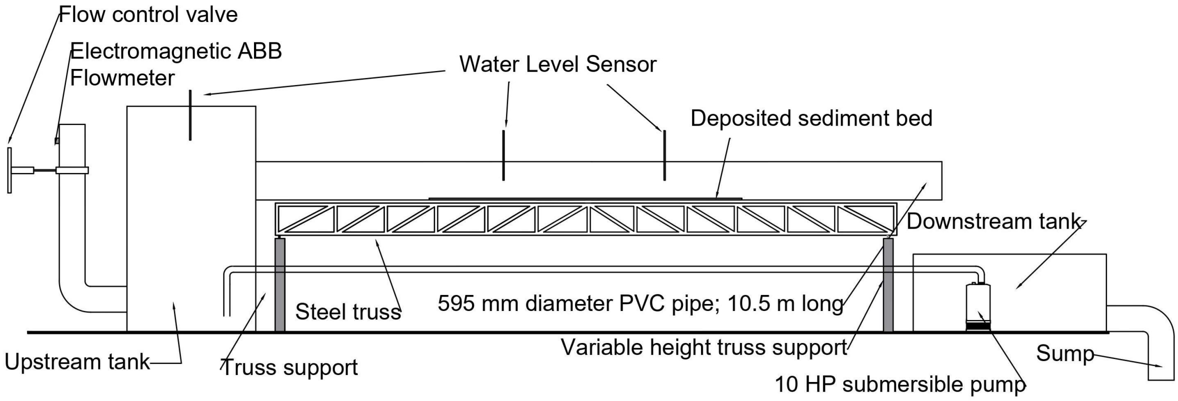

Figure 2. Experimental setup used to collect the unsteady flow data in the 595 mm PVC pipe.

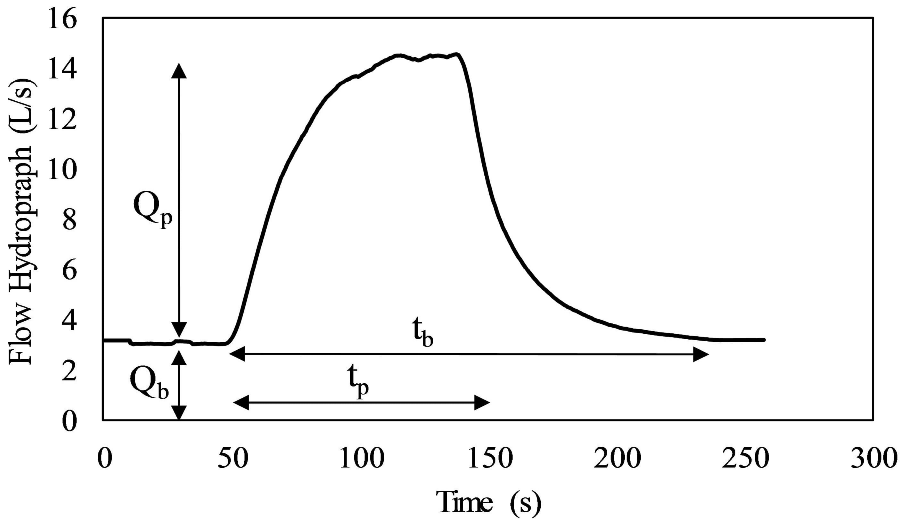

Figure 3. Variable definition of the flushing discharge hydrograph.

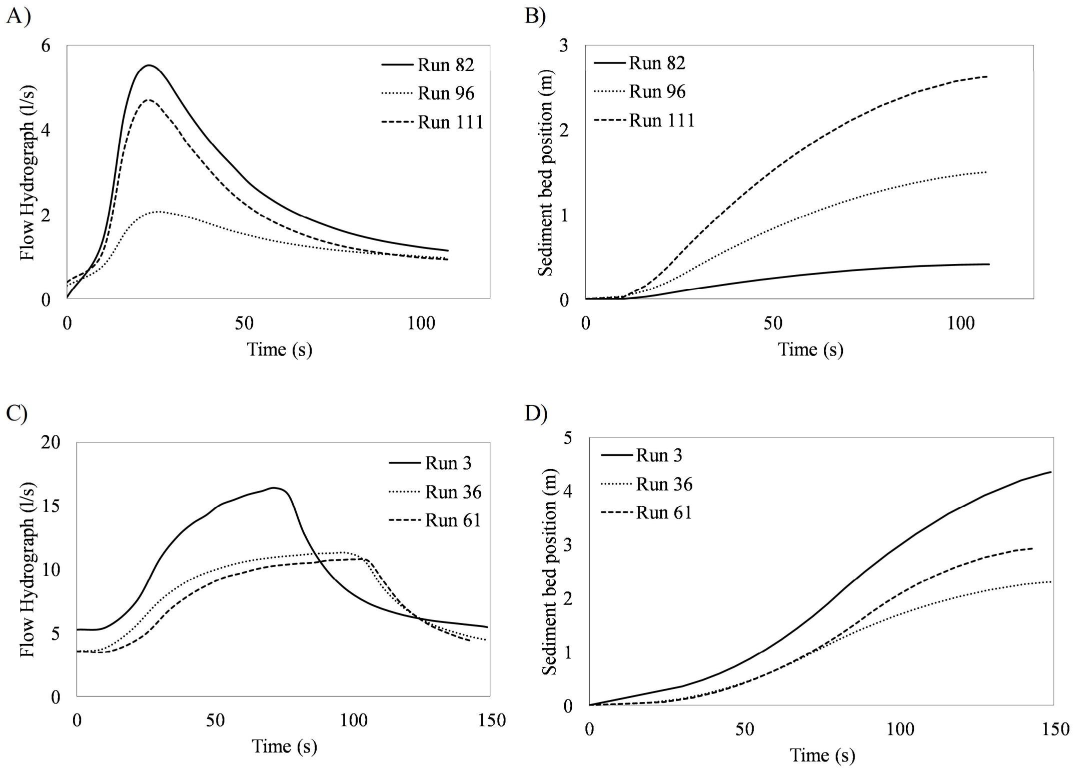

Figure 4. Example of flow hydrographs and sediment bed position for several experiments shown in Table 1.

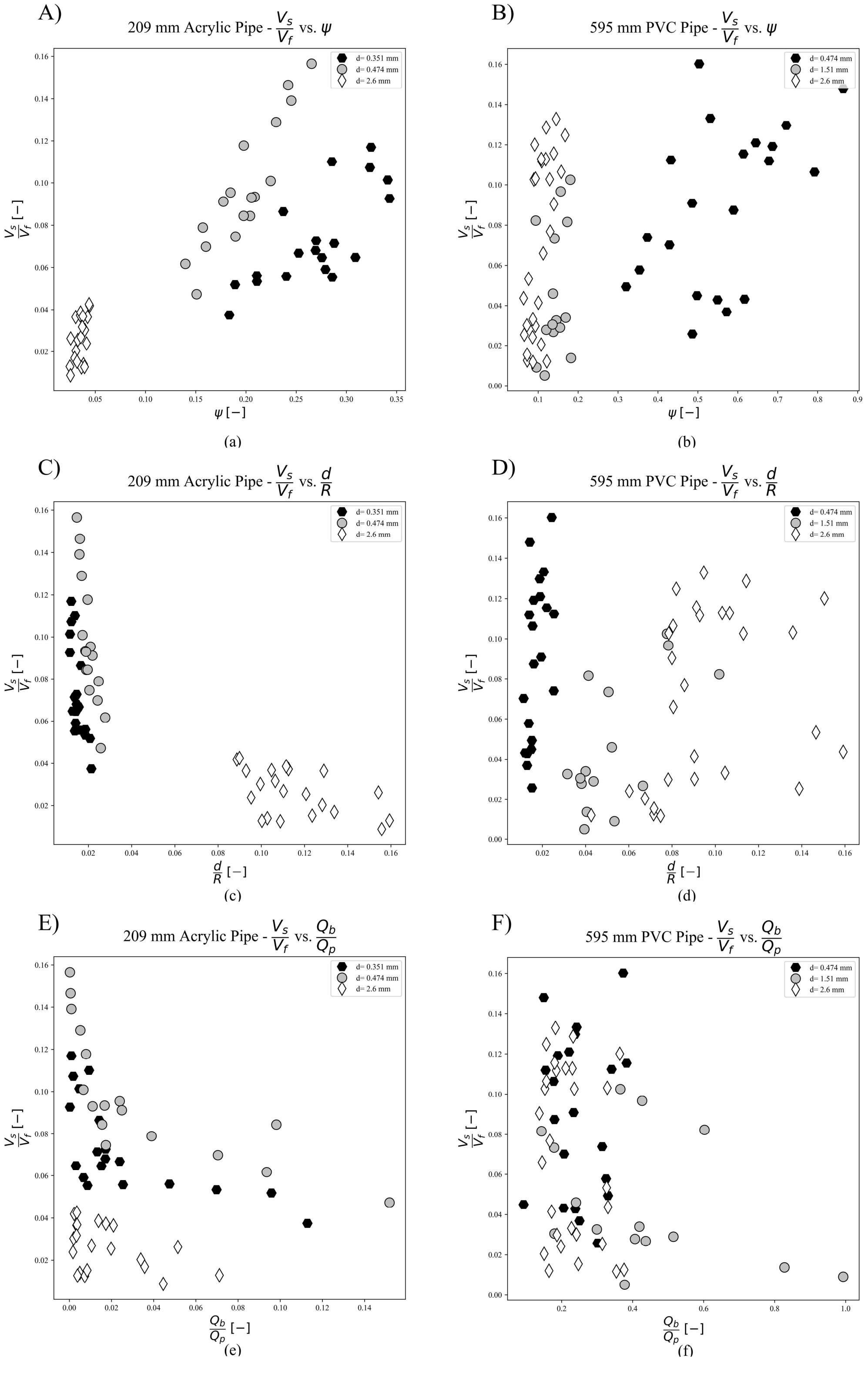

209 mm Acrylic Pipe - $\frac{V_s}{V_f}$ vs. $\psi$

595 mm PVC Pipe - $\frac{V_s}{V_f}$ vs. $\psi$

(a)

(b)

209 mm Acrylic Pipe - $\frac{V_s}{V_f}$ vs. $\frac{d}{R}$

595 mm PVC Pipe - $\frac{V_s}{V_f}$ vs. $\frac{d}{R}$

(c)

(d)

209 mm Acrylic Pipe - $\frac{V_s}{V_f}$ vs. $\frac{Q_b}{Q_p}$

595 mm PVC Pipe - $\frac{V_s}{V_f}$ vs. $\frac{Q_b}{Q_p}$

(e)

(f)

Figure 5. Plots showing the relationships between the dimensionless velocity ($V_s/V_f$) and other dimensionless variables in both acrylic and PVC pipe. Clustered results by particle diameter.

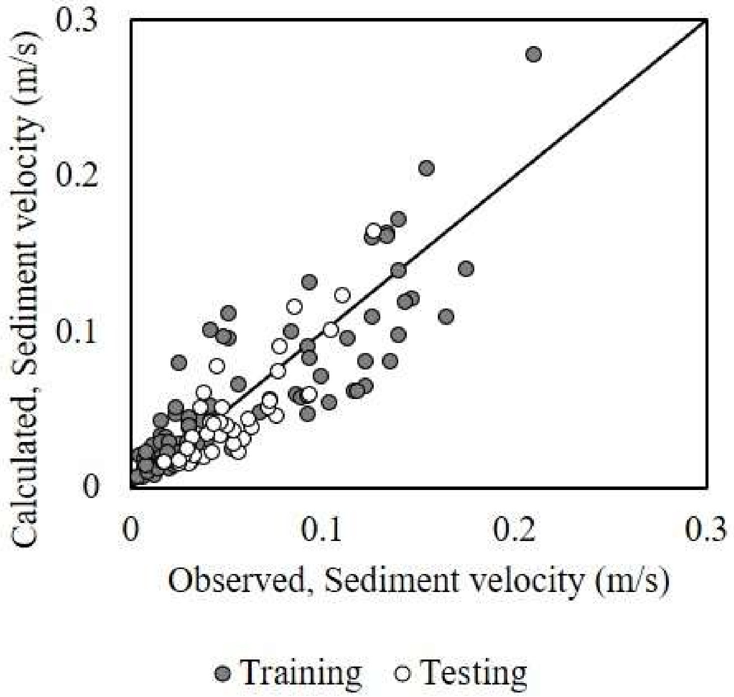

Figure 6. EPR-MOGA model accuracy for both training and testing stage.

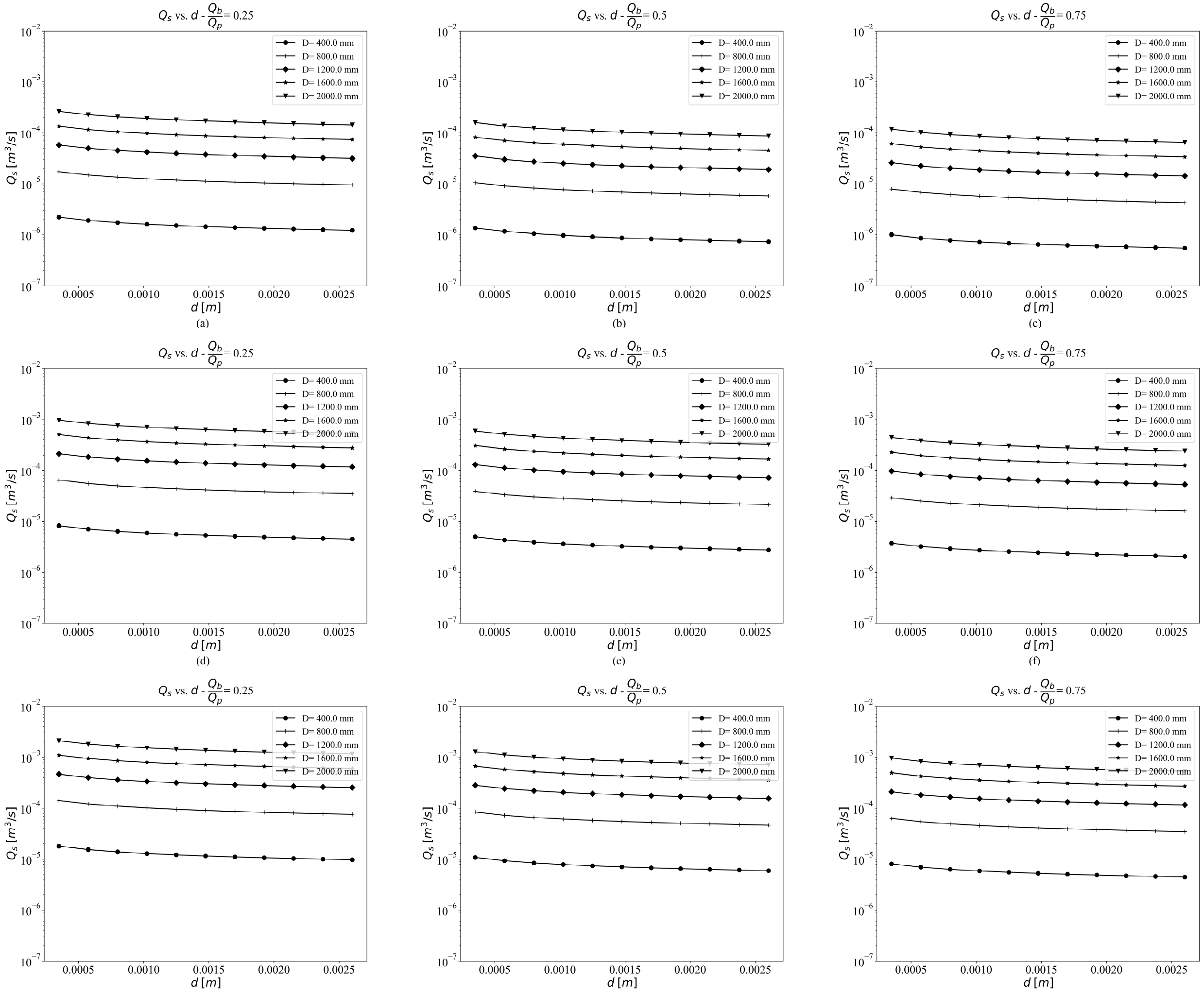

(a) (b) (c)

(d) (e) (f)

Figure 7. Efficiency of flushing discharge vs particle diameter for several base and peak flow relations ($0.25 < Q_b/Q_p < 0.75$) and pipe slope: a), b) and c) $S_o$ = 0.5%; d), e) and f) $S_o$ = 1.0% and g), h) and i) $S_o$ = 1.5%.

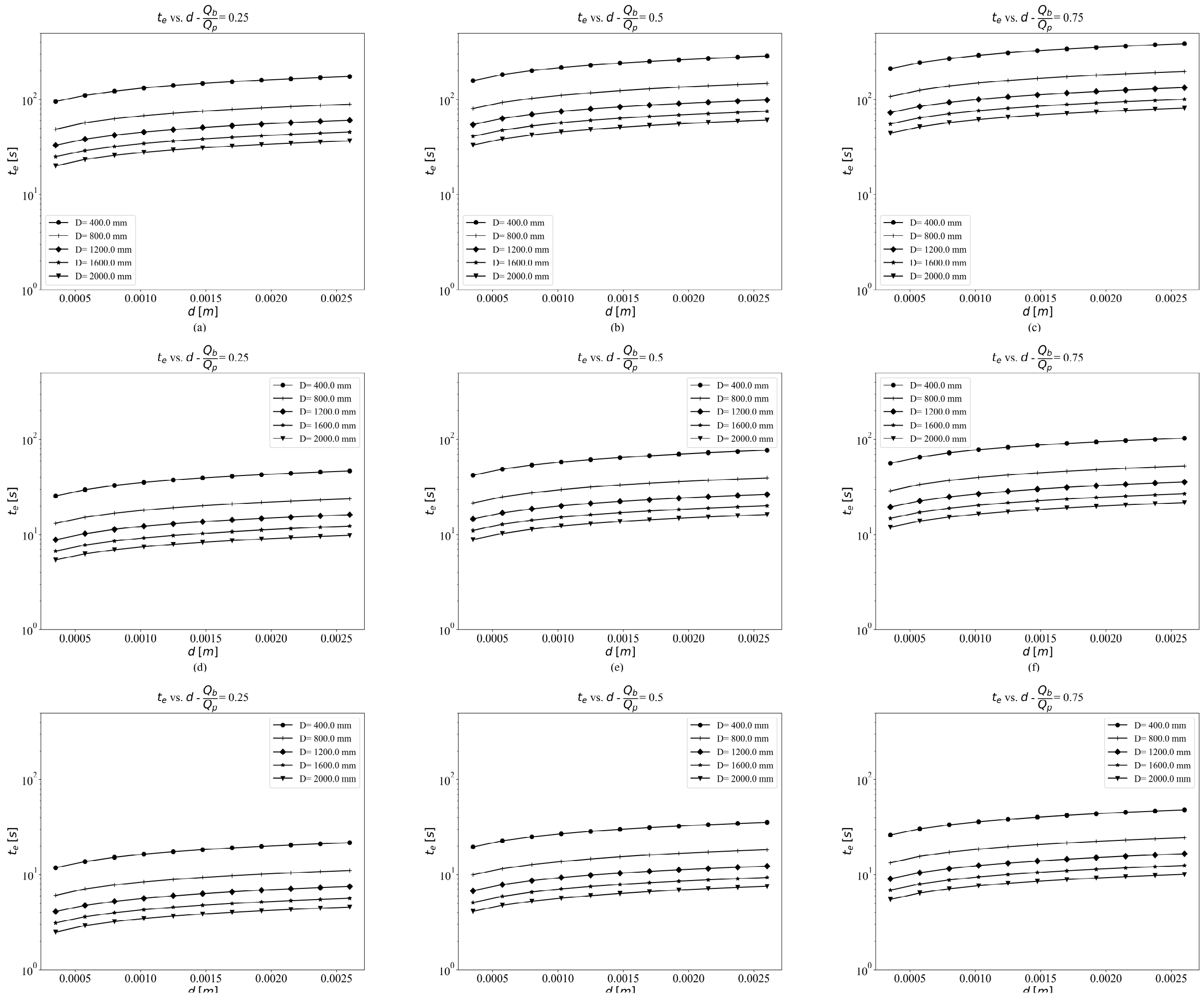

Figure 8. Flushing time vs particle diameter for several base and peak flow relations (0.25 < $Q_b/Q_p$ < 0.75) and pipe slope: a), b) and c) $S_o$ = 0.5%; d), e) and f) $S_o$ = 1.0% and g), h) and i) $S_o$ = 1.5%.

Table 1. Experimental data collected for studying flushing waves efficiency on sewer pipes.

| Run no. | $S_o$ (%) | $D$ (mm) | $Y$ (mm) | $R$ (mm) | $d$ (mm) | $SG$ (-) | $y_s$ (mm) | $t_b$ (s) | $t_p$ (s) | $Q_b$ (l s$^{-1}$) | $Q_p$ (l s$^{-1}$) | $V_f$ (m s$^{-1}$) | $V_s$ (m s$^{-1}$) |
|---|---|---|---|---|---|---|---|---|---|---|---|---|---|
| 1 | 0.805 | 595 | 70.35 | 41.96 | 0.47 | 2.66 | 10.14 | 154 | 59 | 5.27 | 25.48 | 1.02 | 0.07 |
| 2 | 0.805 | 595 | 57.43 | 34.62 | 0.47 | 2.66 | 8.26 | 141 | 57 | 5.45 | 16.76 | 0.89 | 0.05 |
| 3 | 0.805 | 595 | 53.61 | 31.34 | 0.47 | 2.66 | 10.53 | 131 | 57 | 5.45 | 16.49 | 0.82 | 0.04 |
| 4 | 1.186 | 595 | 57.82 | 36.46 | 0.47 | 2.66 | 2.49 | 121 | 59 | 4.89 | 20.53 | 1.20 | 0.05 |
| 5 | 1.229 | 595 | 54.70 | 31.17 | 0.47 | 2.66 | 12.55 | 115 | 55 | 4.81 | 15.97 | 0.99 | 0.03 |
| 6 | 1.229 | 595 | 61.66 | 36.67 | 0.47 | 2.66 | 9.91 | 120 | 55 | 5.07 | 20.27 | 1.14 | 0.04 |
| 7 | 1.229 | 595 | 50.94 | 31.92 | 0.47 | 2.66 | 3.90 | 183 | 58 | 1.03 | 11.10 | 1.09 | 0.05 |
| 8 | 1.229 | 595 | 67.63 | 39.54 | 0.47 | 2.66 | 12.15 | 124 | 57 | 5.03 | 24.47 | 1.19 | 0.05 |
| 9 | 1.229 | 595 | 62.04 | 37.24 | 1.51 | 2.66 | 8.97 | 39 | 33 | 9.98 | 12.06 | 1.16 | 0.02 |
| 10 | 1.525 | 595 | 42.69 | 22.71 | 1.51 | 2.66 | 13.54 | 117 | 58 | 5.17 | 11.84 | 0.87 | 0.02 |
| 11 | 2.034 | 595 | 37.55 | 19.29 | 1.51 | 2.66 | 13.28 | 111 | 59 | 4.92 | 11.54 | 0.89 | 0.09 |
| 12 | 2.331 | 595 | 35.95 | 19.45 | 1.51 | 2.66 | 10.96 | 182 | 57 | 3.99 | 10.93 | 0.97 | 0.10 |
| 13 | 0.763 | 595 | 67.43 | 38.31 | 1.51 | 2.66 | 14.87 | 113 | 56 | 4.42 | 11.71 | 0.90 | 0.00 |
| 14 | 0.763 | 595 | 70.23 | 39.60 | 1.51 | 2.66 | 15.99 | 126 | 69 | 9.13 | 22.46 | 0.92 | 0.03 |
| 15 | 0.763 | 595 | 81.75 | 47.82 | 1.51 | 2.66 | 13.12 | 135 | 63 | 9.40 | 31.43 | 1.07 | 0.04 |
| 16 | 1.123 | 595 | 58.13 | 34.59 | 1.51 | 2.66 | 9.55 | 118 | 60 | 9.23 | 17.93 | 1.04 | 0.03 |
| 17 | 1.123 | 595 | 64.66 | 37.76 | 1.51 | 2.66 | 11.97 | 118 | 57 | 9.37 | 22.36 | 1.10 | 0.04 |
| 18 | 1.186 | 595 | 57.59 | 29.85 | 1.51 | 2.66 | 19.13 | 149 | 79 | 3.59 | 20.04 | 0.92 | 0.07 |
| 19 | 1.186 | 595 | 52.88 | 28.98 | 1.51 | 2.66 | 14.70 | 149 | 88 | 3.95 | 16.45 | 0.91 | 0.04 |
| 20 | 1.186 | 595 | 64.30 | 36.57 | 1.51 | 2.66 | 14.31 | 195 | 93 | 3.51 | 24.52 | 1.09 | 0.09 |
| 21 | 0.847 | 595 | 69.70 | 40.25 | 1.51 | 2.66 | 13.64 | 185 | 55 | 3.72 | 20.71 | 0.99 | 0.03 |
| 22 | 0.847 | 595 | 51.24 | 28.32 | 1.51 | 2.66 | 13.83 | 104 | 8 | 7.28 | 7.33 | 0.76 | 0.01 |
| 23 | 1.589 | 595 | 32.25 | 14.83 | 1.51 | 2.66 | 14.35 | 118 | 82 | 4.36 | 7.24 | 0.65 | 0.05 |
| 24 | 0.847 | 595 | 63.16 | 36.41 | 2.60 | 2.64 | 12.98 | 120 | 76 | 4.71 | 12.53 | 0.92 | 0.01 |
| 25 | 0.847 | 595 | 66.11 | 36.30 | 2.60 | 2.64 | 17.48 | 156 | 86 | 4.10 | 16.57 | 0.90 | 0.01 |
| 26 | 0.847 | 595 | 72.84 | 43.20 | 2.60 | 2.64 | 10.93 | 161 | 83 | 4.13 | 20.88 | 1.06 | 0.03 |
| 27 | 0.847 | 595 | 105.64 | 61.10 | 2.60 | 2.64 | 15.39 | 167 | 65 | 4.11 | 24.98 | 1.34 | 0.02 |
| 28 | 1.059 | 595 | 62.36 | 34.80 | 2.60 | 2.64 | 15.48 | 143 | 75 | 4.22 | 11.91 | 0.99 | 0.01 |
| 29 | 1.059 | 595 | 54.15 | 28.78 | 2.60 | 2.64 | 16.77 | 154 | 83 | 4.02 | 16.63 | 0.85 | 0.03 |
| 30 | 1.186 | 595 | 59.13 | 33.26 | 2.60 | 2.64 | 14.30 | 143 | 67 | 3.69 | 19.77 | 1.01 | 0.03 |
| 31 | 1.186 | 595 | 67.08 | 38.56 | 2.60 | 2.64 | 13.76 | 148 | 74 | 3.57 | 23.71 | 1.14 | 0.02 |
| 32 | 1.483 | 595 | 39.34 | 18.73 | 2.60 | 2.64 | 16.36 | 176 | 88 | 3.45 | 10.96 | 0.73 | 0.02 |

| Run no. | $S_o$ (%) | $D$ (mm) | $Y$ (mm) | $R$ (mm) | $d$ (mm) | $SG$ (-) | $y_s$ (mm) | $t_b$ (s) | $t_p$ (s) | $Q_b$ (l s$^{-1}$) | $Q_p$ (l s$^{-1}$) | $V_f$ (m s$^{-1}$) | $V_s$ (m s$^{-1}$) |
|---|---|---|---|---|---|---|---|---|---|---|---|---|---|
| 33 | 1.483 | 595 | 46.74 | 24.88 | 2.60 | 2.64 | 14.66 | 136 | 80 | 3.52 | 15.45 | 0.91 | 0.03 |
| 34 | 1.483 | 595 | 53.25 | 28.81 | 2.60 | 2.64 | 15.54 | 186 | 72 | 3.39 | 19.73 | 1.01 | 0.04 |
| 35 | 1.483 | 595 | 59.57 | 32.28 | 2.60 | 2.64 | 16.95 | 184 | 79 | 3.42 | 23.61 | 1.10 | 0.07 |
| 36 | 1.653 | 595 | 38.51 | 16.34 | 2.60 | 2.64 | 19.13 | 134 | 82 | 3.75 | 11.36 | 0.69 | 0.03 |
| 37 | 1.653 | 595 | 46.08 | 23.02 | 2.60 | 2.64 | 17.21 | 141 | 84 | 3.76 | 15.96 | 0.90 | 0.09 |
| 38 | 1.653 | 595 | 52.56 | 28.02 | 2.60 | 2.64 | 16.18 | 146 | 70 | 3.71 | 20.08 | 1.04 | 0.12 |
| 39 | 1.653 | 595 | 59.13 | 33.13 | 2.60 | 2.64 | 14.58 | 147 | 64 | 3.64 | 23.79 | 1.19 | 0.12 |
| 40 | 1.568 | 595 | 38.73 | 18.76 | 0.47 | 2.66 | 15.60 | 135 | 87 | 3.64 | 11.58 | 0.76 | 0.06 |
| 41 | 1.568 | 595 | 46.16 | 24.41 | 0.47 | 2.66 | 14.80 | 142 | 81 | 3.73 | 15.96 | 0.92 | 0.08 |
| 42 | 1.568 | 595 | 53.90 | 29.62 | 0.47 | 2.66 | 14.77 | 146 | 87 | 3.66 | 20.35 | 1.07 | 0.09 |
| 43 | 1.568 | 595 | 59.10 | 34.08 | 0.47 | 2.66 | 12.39 | 151 | 81 | 3.75 | 24.25 | 1.20 | 0.13 |
| 44 | 1.822 | 595 | 37.55 | 18.70 | 0.47 | 2.66 | 14.29 | 140 | 87 | 4.06 | 11.92 | 0.82 | 0.09 |
| 45 | 1.822 | 595 | 45.29 | 22.96 | 0.47 | 2.66 | 16.33 | 148 | 88 | 4.00 | 16.48 | 0.95 | 0.13 |
| 46 | 1.822 | 595 | 51.59 | 29.70 | 0.47 | 2.66 | 11.33 | 152 | 81 | 3.95 | 20.87 | 1.17 | 0.14 |
| 47 | 2.034 | 595 | 35.08 | 19.49 | 0.47 | 2.66 | 9.71 | 121 | 84 | 3.97 | 10.64 | 0.92 | 0.15 |
| 48 | 2.034 | 595 | 42.85 | 24.99 | 0.47 | 2.66 | 9.05 | 161 | 89 | 3.26 | 14.75 | 1.11 | 0.13 |
| 49 | 2.034 | 595 | 50.35 | 30.68 | 0.47 | 2.66 | 6.79 | 7 | 78 | 3.56 | 20.07 | 1.32 | 0.14 |
| 50 | 2.034 | 595 | 54.22 | 33.47 | 0.47 | 2.66 | 5.64 | 178 | 60 | 3.56 | 23.79 | 1.42 | 0.21 |
| 51 | 2.246 | 595 | 34.90 | 21.54 | 0.47 | 2.66 | 4.68 | 127 | 75 | 4.36 | 11.38 | 1.09 | 0.13 |
| 52 | 2.246 | 595 | 42.64 | 25.31 | 0.47 | 2.66 | 7.95 | 159 | 77 | 3.78 | 15.90 | 1.19 | 0.15 |
| 53 | 2.246 | 595 | 35.17 | 17.28 | 2.60 | 2.64 | 13.82 | 131 | 78 | 4.07 | 11.19 | 0.86 | 0.10 |
| 54 | 2.246 | 595 | 42.78 | 22.75 | 2.60 | 2.64 | 13.58 | 142 | 88 | 3.62 | 15.55 | 1.06 | 0.14 |
| 55 | 2.246 | 595 | 47.24 | 27.46 | 2.60 | 2.64 | 9.96 | 146 | 85 | 3.62 | 19.82 | 1.24 | 0.17 |
| 56 | 2.246 | 595 | 52.77 | 31.74 | 2.60 | 2.64 | 8.10 | 142 | 79 | 3.72 | 23.74 | 1.40 | 0.18 |
| 57 | 2.076 | 595 | 36.93 | 19.14 | 2.60 | 2.64 | 12.77 | 136 | 85 | 3.90 | 11.87 | 0.90 | 0.09 |
| 58 | 2.076 | 595 | 43.16 | 24.38 | 2.60 | 2.64 | 10.84 | 11 | 77 | 3.69 | 16.02 | 1.09 | 0.12 |
| 59 | 2.076 | 595 | 50.20 | 28.50 | 2.60 | 2.64 | 11.99 | 153 | 92 | 3.67 | 20.34 | 1.21 | 0.14 |
| 60 | 2.076 | 595 | 54.70 | 32.31 | 2.60 | 2.64 | 9.85 | 154 | 79 | 3.79 | 24.16 | 1.35 | 0.14 |
| 61 | 1.822 | 595 | 36.34 | 17.74 | 2.60 | 2.64 | 14.46 | 123 | 84 | 3.54 | 10.84 | 0.79 | 0.04 |
| 62 | 1.822 | 595 | 43.56 | 25.20 | 2.60 | 2.64 | 9.63 | 162 | 85 | 3.20 | 15.12 | 1.05 | 0.12 |
| 63 | 1.822 | 595 | 50.97 | 30.34 | 2.60 | 2.64 | 8.79 | 171 | 78 | 3.18 | 19.05 | 1.21 | 0.09 |
| 64 | 1.822 | 595 | 56.21 | 32.54 | 2.60 | 2.64 | 11.66 | 168 | 87 | 3.25 | 23.71 | 1.25 | 0.11 |
| 65 | 0.644 | 209 | 34.99 | 20.17 | 2.60 | 2.64 | 5.60 | 101 | 18 | 0.08 | 3.80 | 0.55 | 0.02 |
| 66 | 0.644 | 209 | 49.27 | 27.29 | 2.60 | 2.64 | 8.22 | 101 | 16 | 0.01 | 6.60 | 0.68 | 0.02 |

| Run no. | $S_o$ (%) | $D$ (mm) | $Y$ (mm) | $R$ (mm) | $d$ (mm) | $SG$ (-) | $y_s$ (mm) | $t_b$ (s) | $t_p$ (s) | $Q_b$ (l s$^{-1}$) | $Q_p$ (l s$^{-1}$) | $V_f$ (m s$^{-1}$) | $V_s$ (m s$^{-1}$) |
|---|---|---|---|---|---|---|---|---|---|---|---|---|---|
| 67 | 0.644 | 209 | 51.63 | 27.99 | 2.60 | 2.64 | 9.89 | 101 | 14 | 0.02 | 6.84 | 0.68 | 0.02 |
| 68 | 0.644 | 209 | 28.15 | 16.32 | 2.60 | 2.64 | 4.98 | 101 | 20 | 0.14 | 1.99 | 0.48 | 0.01 |
| 69 | 0.644 | 209 | 30.78 | 16.70 | 2.60 | 2.64 | 7.96 | 101 | 19 | 0.11 | 2.45 | 0.47 | 0.00 |
| 70 | 0.644 | 209 | 40.49 | 23.10 | 2.60 | 2.64 | 6.26 | 101 | 17 | 0.08 | 4.73 | 0.61 | 0.02 |
| 71 | 0.644 | 209 | 53.26 | 29.33 | 2.60 | 2.64 | 8.49 | 101 | 15 | 0.02 | 7.37 | 0.71 | 0.03 |
| 72 | 0.644 | 209 | 35.58 | 20.28 | 2.60 | 2.64 | 6.26 | 101 | 20 | 0.12 | 3.62 | 0.55 | 0.01 |
| 73 | 0.644 | 209 | 40.61 | 23.32 | 2.60 | 2.64 | 5.82 | 101 | 18 | 0.06 | 4.58 | 0.62 | 0.02 |
| 74 | 0.644 | 209 | 45.95 | 25.29 | 2.60 | 2.64 | 8.76 | 101 | 17 | 0.03 | 5.42 | 0.64 | 0.01 |
| 75 | 0.644 | 209 | 52.17 | 28.92 | 2.60 | 2.64 | 7.96 | 101 | 16 | 0.03 | 7.22 | 0.71 | 0.03 |
| 76 | 0.644 | 209 | 29.87 | 16.87 | 2.60 | 2.64 | 6.26 | 101 | 21 | 0.11 | 2.06 | 0.48 | 0.01 |
| 77 | 0.644 | 209 | 33.61 | 19.44 | 2.60 | 2.64 | 5.39 | 101 | 19 | 0.10 | 2.75 | 0.54 | 0.01 |
| 78 | 0.644 | 209 | 44.28 | 24.82 | 2.60 | 2.64 | 7.45 | 101 | 18 | 0.02 | 5.17 | 0.64 | 0.02 |
| 79 | 0.644 | 209 | 47.12 | 26.13 | 2.60 | 2.64 | 8.22 | 101 | 18 | 0.01 | 5.90 | 0.66 | 0.02 |
| 80 | 0.644 | 209 | 38.03 | 21.54 | 2.60 | 2.64 | 6.72 | 101 | 19 | 0.08 | 3.80 | 0.58 | 0.01 |
| 81 | 0.644 | 209 | 41.49 | 23.59 | 2.60 | 2.64 | 6.49 | 101 | 18 | 0.05 | 4.59 | 0.62 | 0.02 |
| 82 | 0.644 | 209 | 43.13 | 23.90 | 2.60 | 2.64 | 8.22 | 101 | 17 | 0.04 | 5.55 | 0.61 | 0.01 |
| 83 | 0.644 | 209 | 44.99 | 24.43 | 2.60 | 2.64 | 9.60 | 101 | 16 | 0.02 | 6.11 | 0.62 | 0.02 |
| 84 | 0.644 | 209 | 38.93 | 21.05 | 2.60 | 2.64 | 9.31 | 101 | 18 | 0.04 | 4.51 | 0.55 | 0.01 |
| 85 | 0.644 | 209 | 47.10 | 25.93 | 2.60 | 2.64 | 8.76 | 101 | 17 | 0.02 | 5.83 | 0.65 | 0.01 |
| 86 | 0.644 | 209 | 38.30 | 22.59 | 0.47 | 2.66 | 3.91 | 101 | 17 | 0.10 | 4.36 | 0.62 | 0.06 |
| 87 | 0.644 | 209 | 51.25 | 29.60 | 0.47 | 2.66 | 3.68 | 101 | 16 | 0.00 | 7.36 | 0.76 | 0.11 |
| 88 | 0.644 | 209 | 52.44 | 29.99 | 0.47 | 2.66 | 4.65 | 101 | 15 | 0.01 | 7.64 | 0.75 | 0.10 |
| 89 | 0.644 | 209 | 29.07 | 17.09 | 0.47 | 2.66 | 4.40 | 101 | 19 | 0.21 | 2.22 | 0.50 | 0.03 |
| 90 | 0.644 | 209 | 33.05 | 19.59 | 0.47 | 2.66 | 3.91 | 101 | 17 | 0.19 | 2.65 | 0.56 | 0.04 |
| 91 | 0.644 | 209 | 41.19 | 24.21 | 0.47 | 2.66 | 3.86 | 101 | 18 | 0.04 | 4.99 | 0.65 | 0.08 |
| 92 | 0.644 | 209 | 56.85 | 32.46 | 0.47 | 2.66 | 3.51 | 101 | 15 | 0.00 | 8.02 | 0.81 | 0.13 |
| 93 | 0.644 | 209 | 39.63 | 23.20 | 0.47 | 2.66 | 4.40 | 101 | 17 | 0.07 | 4.08 | 0.62 | 0.05 |
| 94 | 0.644 | 209 | 43.42 | 25.52 | 0.47 | 2.66 | 3.46 | 101 | 17 | 0.08 | 4.99 | 0.68 | 0.06 |
| 95 | 0.644 | 209 | 47.40 | 27.47 | 0.47 | 2.66 | 4.21 | 101 | 16 | 0.04 | 5.56 | 0.71 | 0.07 |
| 96 | 0.644 | 209 | 30.86 | 18.45 | 0.47 | 2.66 | 3.46 | 101 | 19 | 0.32 | 2.08 | 0.54 | 0.03 |
| 97 | 0.644 | 209 | 32.77 | 19.21 | 0.47 | 2.66 | 4.59 | 101 | 20 | 0.11 | 2.80 | 0.54 | 0.04 |
| 98 | 0.644 | 209 | 42.21 | 24.97 | 0.47 | 2.66 | 3.03 | 101 | 19 | 0.41 | 4.22 | 0.67 | 0.06 |
| 99 | 0.644 | 209 | 37.41 | 21.71 | 0.47 | 2.66 | 5.18 | 101 | 19 | 0.09 | 3.79 | 0.59 | 0.05 |
| 100 | 0.644 | 209 | 41.66 | 24.19 | 0.47 | 2.66 | 4.86 | 101 | 17 | 0.07 | 4.63 | 0.64 | 0.05 |

| Run no. | $S_o$ (%) | $D$ (mm) | $Y$ (mm) | $R$ (mm) | $d$ (mm) | $SG$ (-) | $y_s$ (mm) | $t_b$ (s) | $t_p$ (s) | $Q_b$ (l s$^{-1}$) | $Q_p$ (l s$^{-1}$) | $V_f$ (m s$^{-1}$) | $V_s$ (m s$^{-1}$) |
|---|---|---|---|---|---|---|---|---|---|---|---|---|---|
| 101 | 0.644 | 209 | 43.34 | 25.14 | 0.47 | 2.66 | 4.78 | 101 | 18 | 0.06 | 5.71 | 0.66 | 0.06 |
| 102 | 0.644 | 209 | 48.65 | 28.13 | 0.47 | 2.66 | 4.21 | 101 | 16 | 0.03 | 6.67 | 0.72 | 0.09 |
| 103 | 0.644 | 209 | 36.32 | 21.27 | 0.35 | 2.65 | 4.59 | 101 | 18 | 0.06 | 4.24 | 0.58 | 0.05 |
| 104 | 0.644 | 209 | 51.00 | 29.01 | 0.35 | 2.65 | 5.60 | 101 | 15 | 0.01 | 6.81 | 0.73 | 0.08 |
| 105 | 0.644 | 209 | 50.99 | 29.11 | 0.35 | 2.65 | 5.18 | 101 | 15 | 0.01 | 6.90 | 0.73 | 0.09 |
| 106 | 0.644 | 209 | 28.62 | 16.45 | 0.35 | 2.65 | 5.39 | 101 | 18 | 0.23 | 2.00 | 0.48 | 0.02 |
| 107 | 0.644 | 209 | 32.66 | 18.92 | 0.35 | 2.65 | 5.26 | 101 | 17 | 0.19 | 2.67 | 0.53 | 0.03 |
| 108 | 0.644 | 209 | 42.79 | 24.72 | 0.35 | 2.65 | 5.18 | 101 | 16 | 0.07 | 4.80 | 0.65 | 0.04 |
| 109 | 0.644 | 209 | 54.41 | 30.76 | 0.35 | 2.65 | 5.60 | 101 | 17 | 0.00 | 7.36 | 0.76 | 0.07 |
| 110 | 0.644 | 209 | 37.13 | 21.55 | 0.35 | 2.65 | 5.18 | 101 | 18 | 0.10 | 3.75 | 0.59 | 0.03 |
| 111 | 0.644 | 209 | 41.56 | 24.21 | 0.35 | 2.65 | 4.59 | 101 | 17 | 0.08 | 4.71 | 0.64 | 0.05 |
| 112 | 0.644 | 209 | 45.08 | 25.81 | 0.35 | 2.65 | 5.73 | 101 | 17 | 0.07 | 5.47 | 0.67 | 0.05 |
| 113 | 0.644 | 209 | 54.08 | 30.60 | 0.35 | 2.65 | 5.60 | 101 | 15 | 0.03 | 7.31 | 0.76 | 0.08 |
| 114 | 0.644 | 209 | 29.46 | 16.96 | 0.35 | 2.65 | 5.39 | 101 | 20 | 0.19 | 2.02 | 0.49 | 0.03 |
| 115 | 0.644 | 209 | 33.04 | 18.92 | 0.35 | 2.65 | 5.90 | 101 | 19 | 0.13 | 2.74 | 0.53 | 0.03 |
| 116 | 0.644 | 209 | 44.81 | 25.64 | 0.35 | 2.65 | 5.82 | 101 | 17 | 0.04 | 5.18 | 0.66 | 0.04 |
| 117 | 0.644 | 209 | 48.43 | 27.71 | 0.35 | 2.65 | 5.39 | 101 | 17 | 0.02 | 5.88 | 0.70 | 0.05 |
| 118 | 0.644 | 209 | 39.31 | 22.65 | 0.35 | 2.65 | 5.60 | 101 | 18 | 0.09 | 3.92 | 0.60 | 0.04 |
| 119 | 0.644 | 209 | 41.99 | 24.16 | 0.35 | 2.65 | 5.60 | 101 | 17 | 0.08 | 4.59 | 0.63 | 0.04 |
| 120 | 0.644 | 209 | 43.59 | 25.04 | 0.35 | 2.65 | 5.60 | 101 | 18 | 0.04 | 5.64 | 0.65 | 0.04 |
| 121 | 0.644 | 209 | 44.65 | 25.62 | 0.35 | 2.65 | 5.60 | 101 | 17 | 0.06 | 6.12 | 0.66 | 0.07 |

Table 2. Pareto solution provided by the EPR-MOGA strategy.

| **Number of Inputs** | **Terms of monomial formula** | | | | | | | **Performance Index** | |
|---|---|---|---|---|---|---|---|---|---|
| | **Coefficient ($a_j$)** | $\psi$ | $\frac{Q_b}{Q_p}$ | $\frac{d}{R}$ | $\frac{y_s}{R}$ | $\frac{t_b}{t_p}$ | $\beta$ | $BIC$ | $R^2$ |
| 1 | 0.17 | 0.50 | - | - | - | - | - | -48.21 | 0.38 |
| 2 | 0.14 | 0.60 | -0.10 | - | - | - | - | -66.19 | 0.48 |
| 3 | 8.13 | 1.40 | -0.30 | 0.90 | - | - | - | -104.55 | 0.63 |
| 4 | 11.47 | 1.50 | -0.30 | 1.00 | 0.10 | - | - | -100.56 | 0.64 |
| 5 | 121.48 | 2.10 | -0.20 | 1.60 | 0.80 | 0.10 | - | -96.49 | 0.64 |
| 6 | 2.48 | 1.40 | -0.30 | 0.90 | 0.10 | -0.20 | 1.00 | -92.22 | 0.64 |

Table 3. Comparison of results for predicting the flushing efficiency in Laplace et al. (2003) case of study.

| **Reference** | **Removal rate [kg m$^{-3}$]** | **Observations** |
|---|---|---|
| Laplace et al. (2003) | 0.93 | Original case of Study reported in a trunk combined sewer in Marseille, France |
| Dettmar (2007) | - | Volume of water value reported to clean a pipe section of 150 m long. Relevant parameters as pipe slope and particle diameter are not considered. |
| Bong et al. (2013) | 0.21 | Good approximation. Experimental model (Eq. (3)) obtained with a constant flume slope of 0.001. |
| EPR-MOGA Eq. (10) | 0.4 – 1.25 | Good performance for predicting the removal rate during flushing waves operation. Model consider relevant parameters as the mean particle diameter and the pipe geometry. |